A Solution Rheology Approach to Component Dynamics in A/B Miscible Blends. 2. Friction Coefficients of Polymers A and B

Xiaoping Yang,[†,‡] Adel Halasa,[‡] Wen-Liang Hsu,[‡] and Shi-Qing Wang*[,†]

Department of Macromolecular Science and Engineering, Case Western Reserve University, Cleveland, Ohio 44106, and Goodyear Research Center, Akron, Ohio 44305

Received November 10, 2000; Revised Manuscript Received August 20, 2001

ABSTRACT: A solution rheology method has been applied to resolve component friction dynamics in polymer mixtures. The approach consists of separately evaluating viscoelastic properties of entangled "object" solutions of polymeric A in oligomeric B and "mirror" solutions of polymeric B in oligomeric A. At various compositions, the friction coefficients ζ_A and ζ_B associated with both components A and B are obtained by applying the well-established reptation theory to analyze the oscillatory shear measurements of storage and loss moduli of these object and mirror solutions. It is found that $\zeta_A(\phi,T)$ and $\zeta_B(\phi,T)$ exhibit different temperature and composition dependencies. Specifically, the low-T_g component A, which is low vinylbutadiene (1,4-PB) in the present case, has considerably weaker temperature and composition dependencies in comparison with the high-T_g component B, which is a high vinyl butadiene (1,2-PB). Further analysis indicates the presence of two consecutive glass transitions in the mixtures. A revised free volume theory (FVT) is proposed to assign different levels of free volume to the components in a mixture as the origin of the separable glass transitions.

I. Introduction

When both components of a miscible A/B polymer blend have a comparable level of chain entanglement, they can have equally important contributions to the overall rheological properties. The second factor influencing the component dynamics are the friction coefficients ζ_A and ζ_B associated with each type of chain segment. If ζ_A has a significantly different temperature dependence from that of ζ_B, breakdown of the time−temperature superposition (tTs) principle may be observable. Detailed viscoelastic measurements do not necessarily allow a clear identification of each component dynamics. Besides the interesting question of how ζ_A and ζ_B differ from each other, it is essential to determine how each vary with composition and temperature.

In a recent paper,[1] we have described a solution rheology approach (SRA) to indirectly evaluate the component dynamics in entangled blends using rheological (viscoelastic) measurements. In that publication,[1] we illustrated the potential usefulness of the method and showed how the composition and temperature dependence of the friction coefficient $\zeta_A(\phi,T)$ can be evaluated rheologically in an entangled solution of polymer A. The SRA applies the well-established tube-reptation model of de Gennes−Doi−Edwards[2,3] to describe the linear viscoelastic properties of entangled polymer solutions. Three simple modifications of the original reptation theory included (a) a concentration-dependent tube diameter $a(\phi)$, (b) a Rouse segmental friction coefficient $\zeta_A(\phi,T)$, and (c) a plateau modulus $G_N^0(\phi)$ proportional to the volume fraction ϕ of polymer A and inversely proportional to the square of the tube diameter $G_N^0(\phi) \propto \phi/[a(\phi)]^2$. The relaxation time τ_A for disentanglement of a chain of length N depends on ζ_A according to $\tau_A \propto \zeta_A(\phi,T)N^3/k_BT[a(\phi)]^2$. The idea of SRA is to immerse long chains of polymer A in short chains of oligomer B to form entangled solutions and to measure τ_A at different composition ϕ of polymer A to obtain $\zeta_A(\phi,T)$. Similarly, $\zeta_B(\phi,T)$ can be determined by preparing entangled solutions consisting of long B chains in short chains of oligomeric A and measuring τ_B.

In the literature thermorheological complexity or breakdown of the tTs in real blends has often been assumed to originate from concentration fluctuations.[4−8] The basic assumption in concentration fluctuation theory (CFT) is that concentration fluctuations induce dynamic microscopic heterogeneity that relaxes more slowly than segmental relaxation. More recently, Kumar, Colby, and co-workers[9] have proposed a modified version of CFT and quantitatively explained the existing experimental data on miscible PI/PVE blends obtained through dielectric spectroscopy.[10] On the other hand, an attempt has also been made to describe individual component dynamics in a polymer blend using a "self-concentration" concept.[11] The NMR study[12] supports the idea that the component dynamics are more distinguishable on a more local length scale. In the present work, we focus on component dynamics on large scales and evaluate the friction coefficients associated with the terminal relaxation dynamics in polymer solutions containing polymeric A (or B) and oligomeric B (or A).

In this paper, we use SRA to measure friction coefficients of a pair of "object" and "mirror" systems, based on 1,4-polybutadiene (1,4-PB), 1,2-polybutadiene (1,2-PB), and their oligomeric counterparts (1,4-oBD and 1,2-oBD, respectively). Friction coefficients of 1,4- and 1,2-PB are determined rheologically at various temperatures and different compositions by preparing two sets of solutions (1,4-PB in 1,2-oBD and 1,2-PB in 1,4-oBD). We find that $\zeta_A(\phi,T)$ and $\zeta_B(\phi,T)$ have significantly different composition and temperature dependences. Further analysis indicates that each component undergoes a glass transition at a different temperature. This

[†] Case Western Reserve University.
[‡] Goodyear Research Center.
* Corresponding author. Present address: Department of Polymer Science, University of Akron, Akron, OH 44325.

10.1021/ma0019306 CCC: $20.00
Published on Web 10/19/2001

Table 1. Characteristics of PBs and Oligomeric Butadienes

	microstructure (%)					
sample	cis-1,4	trans-1,4	vinyl	M_w	M_n	MWD
1,4-PB	35	55	10	240000	205000	1.19
1,2-oBD1			82		1000	
1,2-PB			82	231000	225000	1.03
1,4-oBD1	35	55	10		1000	
1,2-oBD2			82	4000	3900	1.03

suggests a simple modification of the free volume theory that allows the different components in a miscible blend to have different levels of free volume in a common microenvironment. Our experimental results support the tentative conclusion reached previously for a polymer blend of similar components[13] and offer information beyond that obtained with traditional rheological measurements because the SRA inherently avoids the thermorheological complexity.

II. Experimental Section

Materials. Both the 1,4- and the 1,2-polybutadienes and their oligomers were synthesized and characterized in the Goodyear Research Center. Table 1 shows the molecular characteristics of all the samples.

As shown in Table 1, the polymeric butadienes have the same microstructures as the corresponding oligomeric butadienes. The oligomeric butadienes' molecular weights are below their entanglement molecular weights (M_e = 1600 for 1,4-PB and 3700 for 1,2-PB). Mixtures of 1,4-PB with oligomer 1,2-butadiene (1,2-oBD1) were prepared with polymer weight fractions equal to 75%, 50%, and 25%, respectively. For reasons that will be clear later, we call these mixtures of 1,4-PB in 1,2-oBD1 "object" systems. Mixtures of 1,2-PB immersed in 1,4-oBD1 are also prepared with polymer weight fractions of 75%, 50%, and 25% and will be termed "mirror" systems. All of these mixtures are prepared by dissolving known amounts of polymer and oligomer in toluene and stirring frequently to promote mixing. Normally, the dissolving process takes about 2−3 days. After achieving a uniform solution, the sample is placed into a vacuum oven to remove toluene at room temperature until the sample contains less than 0.2% of toluene. The whole process takes about a week or so.

Apparatus. Linear viscoelastic properties of the PB solutions are measured using a dynamic mechanical spectrometer (Rheometrics RMS-800) at frequencies ranging from 0.05 to 100 rad/s and temperatures from 80 to −80 °C. The spectrometer is equipped with a 200−2000 g cm dual range force rebalance transducer. The oscillatory shear measurements are carried out using 8 mm diameter parallel plates for the pure polymer and the 75%, 50% polymer solutions. A pair of 25 mm diameter parallel plates were used to obtain the viscoelastic properties for the solutions containing 25% polymer to bring the signal intensity into the machine's sensitivity range.

The glass transition temperatures of both pure polymers and the solutions were measured with a modulated DSC (DSC 2920 from TA instruments) using sample weights in the range 25−30 mg. The samples are first cooled to −140 °C and equilibrated for 10 min. The measurements are taken by heating the samples at 10 °C/min.

III. Results and Discussions

Glass Transition Temperatures Measured by DSC. The glass transition behavior of the object and mirror solutions are measured by DSC and shown in Figure 1a,b. Compared to the pure polymers and oligomers, the glass transitions of the solutions are more gradual and the widths of the transitions are broader especially at higher concentrations of the high T_g component. Note that both 75% 1,4- and 75% 1,2-solutions have the smallest concentration fluctuations

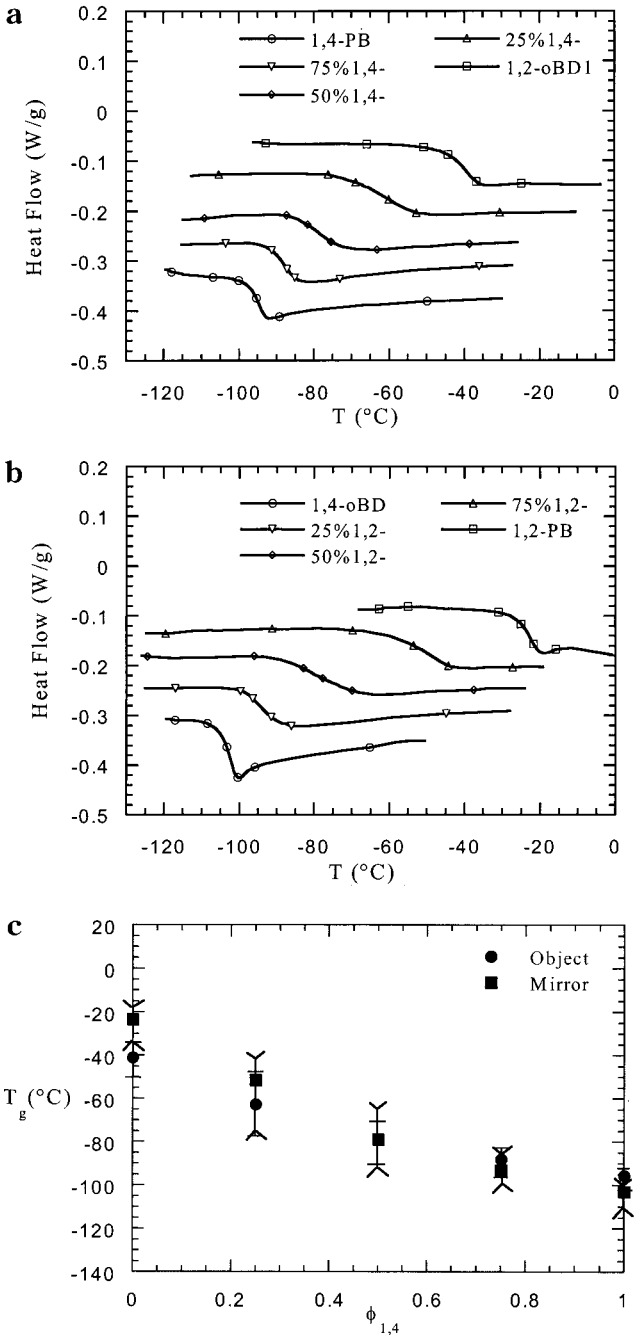

Figure 1. (a) DSC traces of 1,4-PB, 1,2-oBD1, and their solutions (object systems). (b) DSC traces of 1,2-PB, 1,4-oBD1, and their solutions (mirror systems). (c) The glass transition temperatures of both object and mirror solution systems as a function of 1,4-concentration.

according to their static structure factors $S(0) < 5$, which is calculated from $1/S(0) = 1/\phi_1 N_1 + 1/\phi_2 N_2 - 2\chi$ using the value for χ used in ref 13, where ϕ_i and N_i are the concentration and length of the component i, respectively. However, one has the narrowest and the other has the broadest glass transition among their respective series, each consisting of three solutions. Thus, it appears that concentration fluctuations may not be the origin of the transition broadening. The inflection point of the heat flow curve is taken as the glass transition temperature. In Figure 1c, we compare the glass transition temperatures of the object and mirror systems as functions of 1,4-composition. The error bars associated with each point indicate the width of the transition.

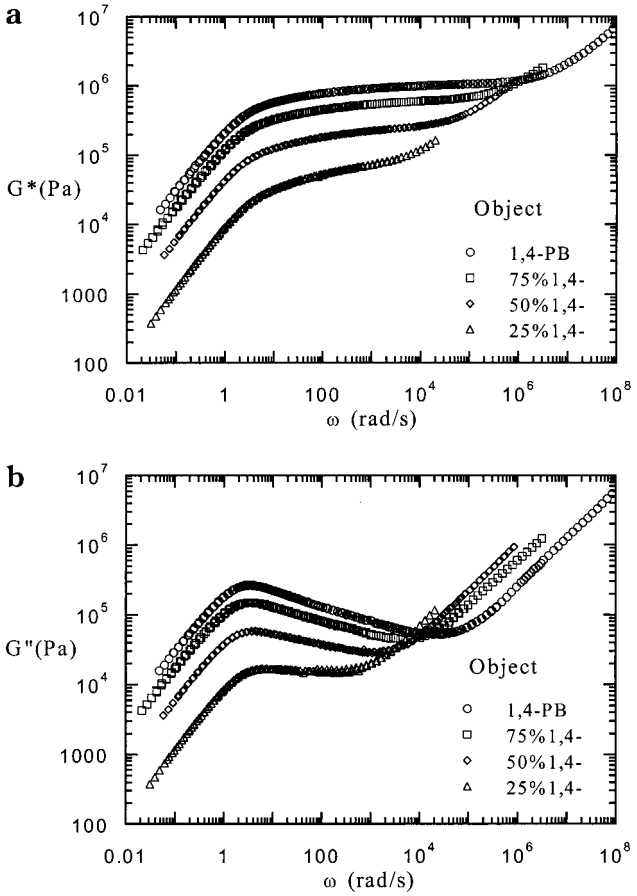

Figure 2. Master curves of (a) the complex moduli and (b) the loss moduli of the object solution systems as a function of the oscillation frequency.

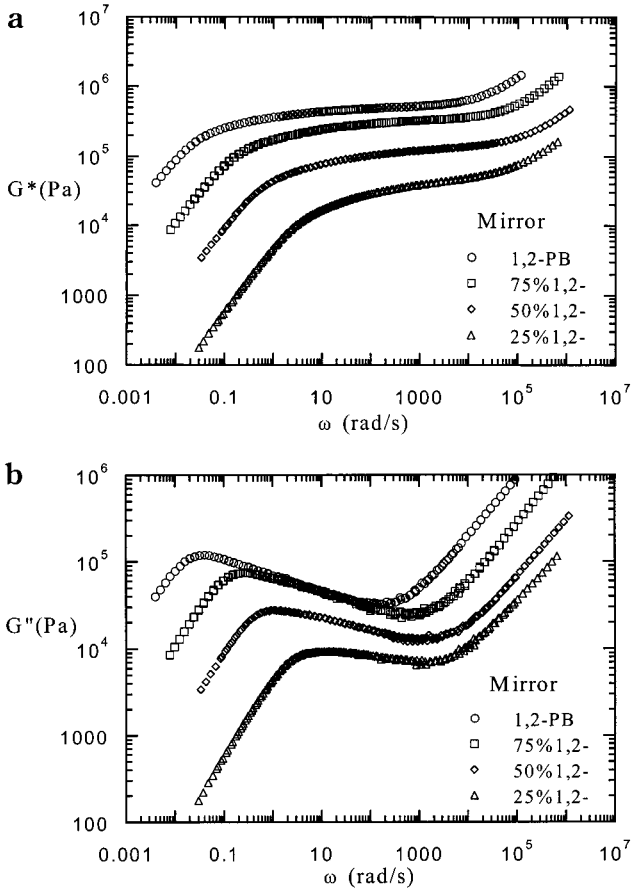

Figure 3. Master curves of (a) the complex moduli and (b) the loss moduli of the mirror solution systems as a function of the oscillation frequency.

For each composition, $T_g(\phi)$ of the object and mirror solutions are essentially the same within the error bars.

Viscoelastic Characteristics of Entangled Solutions. The dynamics of highly entangled polymer solutions can be described by modifying the well-established tube reptation model for linear viscoelastic properties of entangled melts.[1] Figures 2 and 3 show the master curves of the complex moduli and loss moduli of the object and mirror solutions as functions of the oscillation frequency at a reference temperature of 40 °C. Because the polymers in these solutions dominate the viscoelastic behavior, time−temperature superposition holds well as indicated by the high quality of these master curves in terms of the smoothness and connectivity. A single peak is observed in the loss modulus at all concentrations, indicating a single dominant relaxation process in each solution. The characteristics shown in Figure 2a,b are similar to those reported before,[1] where the maximum of G'' stays almost constant with respect to the composition in this object system involving 1,4-PB in 1,2-oBD. On the contrary, the mirror solutions behave differently as expected, with the maximum in G'' shifting strongly with the composition.

The scaling of the plateau modulus for the object and mirror systems is similar, with $G_N^0(\phi) \propto \phi^{2.1\pm0.2}$. This scaling of the plateau modulus is consistent with our previous finding[1] within the experimental uncertainty. Since $G_N^0(\phi)$ is related to the tube diameter $a(\phi)$ according to $G_N^0(\phi) \propto \phi/[a(\phi)]^2$ as discussed before,[1] we will assume the scaling of $a(\phi) \propto \phi^{-0.65}$ to evaluate the friction coefficients $\zeta_A(\phi,T)$ and $\zeta_B(\phi,T)$ from the terminal relaxation (reptation) times $\tau_i \propto \zeta_i(\phi,T)N^3/k_BT[a(\phi)]^2$, where in what follows $i = 1,4$ stands for the 1,4-component and $i = 1,2$ for the 1,2-component. Below a subscript "0" will be used to denote quantities for the pure components.

Reptation Times and Friction Coefficients. For linear monodisperse polymer melts and concentrated solutions the reptation time τ_d can be taken from the master curve as the reciprocal of the crossover frequency ω^* for which $G'(\omega^*) = G''(\omega^*)$. In object solutions, the oligomeric 1,2-butadiene swells the tube diameter and speeds up the relaxation rate of the long 1,4-polybutadiene. On the other hand, because of the higher T_{g0} of 1,2-oBD, the 1,4-PB chains experience a larger segmental friction coefficient. These two factors, tube dilation and "deplastization", compete to affect the overall relaxation time of 1,4-PB chains. Figure 4a shows the reptation time of the object solutions relative to that of the pure 1,4-PD at different temperatures as a function of composition. At lower temperatures (i.e., below room temperature), the reptation times τ_d in the solutions are longer than that of the pure 1,4-PB, τ_{d0}, indicating that deplastization overwhelms the tube dilation effect as expected. Using the assumed scaling of $a(\phi) \propto \phi^{-0.65}$, we obtain the ratio of the friction coefficients as shown in Figure 4b. This ratio is always larger than unity and increases as the composition of 1,2-butadiene, $\phi_{1,2} = 1-\phi_{1,4}$, increases, demonstrating the dynamic influence of the 1,2-oligomeric component on the dispersed long chains. This is anticipated from the rising glass transition temperature of the object solutions relative to that of the pure 1,4-PB as shown in Figure 1c.

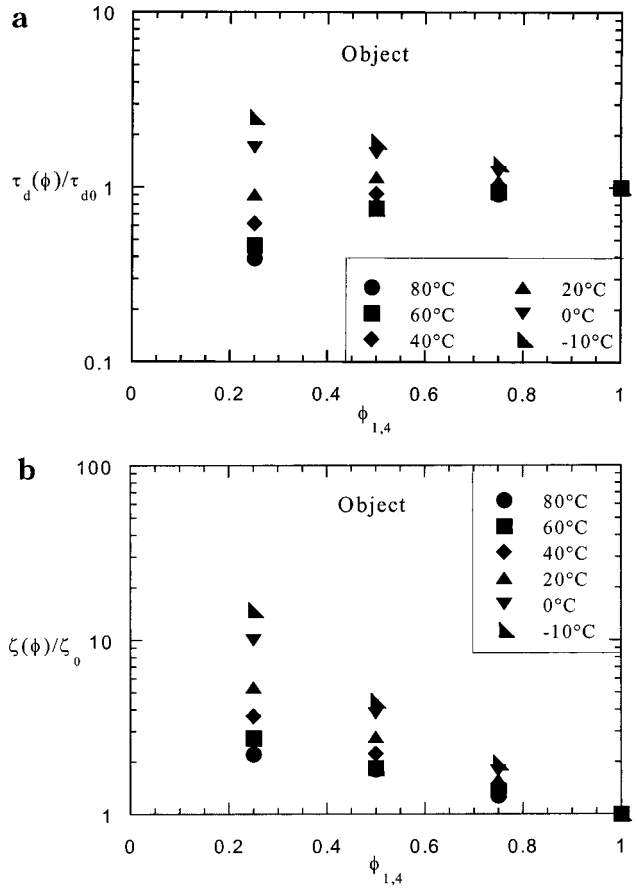

Figure 4. (a) Normalized terminal relaxation times and (b) normalized segmental friction coefficients of the object solution systems as a function of the 1,4-PB concentration at 80, 60, 40, 20, 0, and −10 °C.

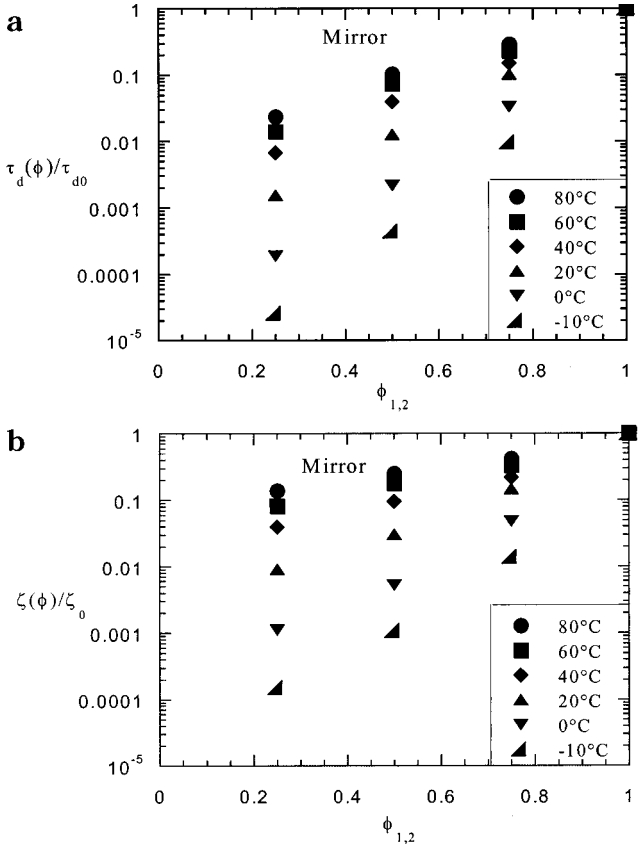

Figure 5. (a) Normalized terminal relaxation times and (b) normalized segmental friction coefficients of the mirror solution systems as a function of the 1,2-PB concentration at 80, 60, 40, 20, 0, and −10 °C.

In the mirror solutions, the same tube dilation takes place. Moreover, the oligomeric 1,4-butadiene "solvent" plasticizes 1,2-PB chains, causing the reptation time to shorten rapidly relative to that of the pure 1,2-PB. The speedup is even faster at low temperatures as shown in Figure 5a. Figure 5b shows that the friction coefficient ζ associated with the 1,2-component is always smaller than ζ_0 of the pure 1,2-PB and increases toward ζ_0 as the 1,2-PB concentration increases.

Comparison of Two Friction Coefficients. Up to now, only ratios of the friction coefficients (relative to the pure components) have been evaluated. To make a direct comparison of the component dynamics, we need to obtain the absolute value of each friction coefficient as a function of composition and temperature. Taking the tube diameter a and the entanglement molecular weight M_e for pure 1,4- and 1,2-PB from the literature,[14] the friction coefficients $\zeta_{01,4}$ and $\zeta_{01,2}$ of the pure 1,4-PB and pure 1,2-PB can be calculated from the absolute values of relaxation times of the pure 1,4-PB and 1,2-PB, $\tau_{01,4}$ and $\tau_{01,2}$, respectively. Specifically, the tube diameters a_0 of 1,4-PB and 1,2-PB with such microstructures as described in Table 1 are 37.5 and 49.7 Å, respectively. Using the standard formula $\tau_0 = \zeta_0 N^3 a_0^2/\pi^2 k_B T N_e^2$, where $N = M_w/m$ and $N_e = M_e/m$ with $m =$ 54 g/mol, we calculate ζ_0 at different temperatures for both pure 1,4-PB and 1,2-PB, assuming a_0 stays nearly constant with T. Figure 6a shows the comparison between the two components.

Having evaluated $\zeta_{01,4}$ and $\zeta_{01,2}$ in Figure 6a, we can refer to Figures 4b and 5b to obtain $\zeta_{1,4}$ and $\zeta_{1,2}$ explicitly. In Figure 6b−d, we compare the friction coefficients of 1,4-PB and 1,2-PB at the 1,4 compositions of 75%, 50%, and 25%. For all the compositions, the friction coefficient of 1,4-PB is significantly below that of 1,2-PB at any given temperature. Furthermore, the separation between the two coefficients increases as temperature decreases toward the glass transition temperature. In other words, the two friction coefficients appear to have different temperature dependencies. This can be more explicitly shown in Figure 7 in terms of the ratio of the two friction coefficients at different temperatures and compositions. At a given temperature, the larger ratio at a lower 1,4-composition essentially stems from the fact that the mixtures are closer to their glass transition temperature. Thus, when plotting the ratio against the distance from T_g^{DSC}, i.e., against $T - T_g^{DSC}$, as shown by the inset in Figure 7, the three curves approximately form a master curve. Here T_g^{DSC} is the mean value of the glass transition temperature given in Figure 1c determined from DSC. The lack of perfect overlap suggests that T_g^{DSC} may not be a common glass transition temperature to both components. Below we carry out additional analysis to better characterize the individual component dynamics.

IV. Further Data Analysis and New Free Volume Theory

Data Analysis. We expect the temperature dependence of $\zeta_{1,4}$ and $\zeta_{1,2}$ to follow a WLF-type equation

$$\log \frac{\zeta(\phi,T)}{\zeta_g(\phi)} = -\frac{c_1[T - T_g(\phi)]}{c_2 + T - T_g(\phi)} \qquad (1)$$

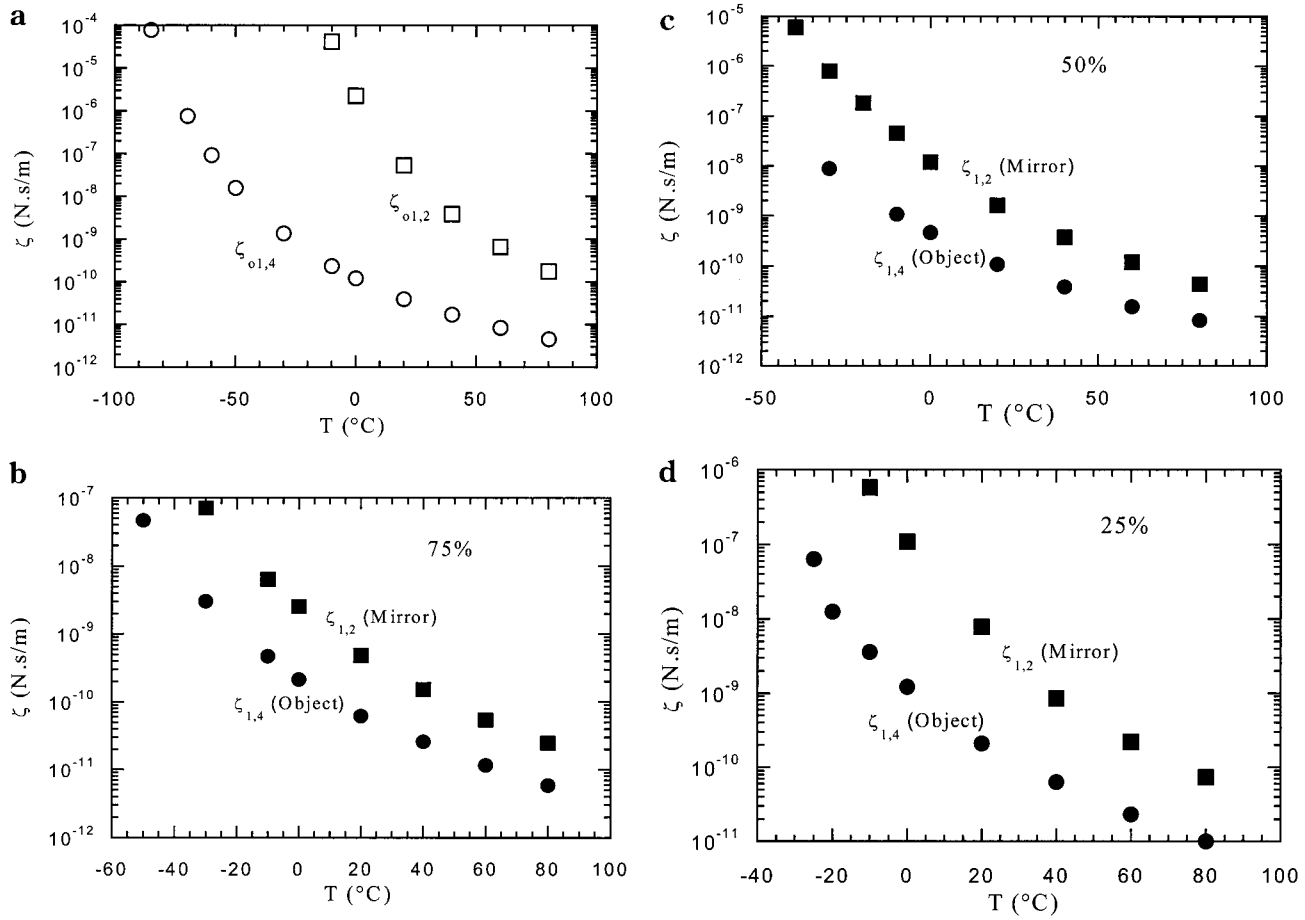

Figure 6. (a) Friction coefficients of pure 1,4-PB and 1,2-PB as a function of temperature. (b), (c), and (d) show temperature dependence of friction coefficients of 1,4-PB and 1,2-PB in object and mirror solutions at compositions 1,4:1,2 = 75%, 50%, and 25%, respectively. In (a)−(d) the unit for the friction coefficients is N s/m.

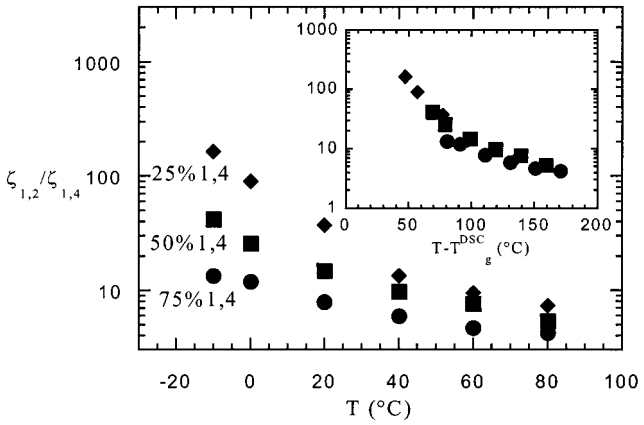

Figure 7. Ratios of the segmental friction coefficients of 1,4-PB and 1,2-PB obtained from the object and mirror solutions with compositions equal to (a) 1,4:1,2 = 75%, (b) 1,4:1,2 = 50%, and (c) 1,4:1,2 = 25%. The inset shows the collapsed data when plotted against the distance from T_g^{DSC}.

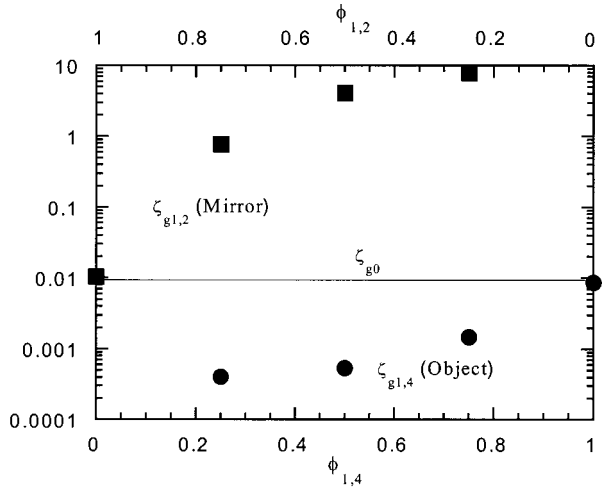

Figure 8. Friction coefficients of 1,4-PB and 1,2-PB evaluated from component dynamics of object and mirror systems at the glass transition temperatures T_g^{DSC} determined by the DSC, where ζ_{g0} denotes the approximate value for the pure components, in the unit of N s/m. The squares obtained from the mirror solutions should be read with respect to the composition $\phi_{1,2}$ of 1,2-PB at the top abscissa. The circles are from the object system with respect to $\phi_{1,4}$ of 1,4-PB at the lower abscissa.

For a given composition, we have two choices to fit the data in Figure 6a−d. The first method is to use the value of T_g^{DSC} determined from the DSC as $T_g(\phi)$ in eq 1 and allow c_1, c_2, and ζ_g to be adjustable. The fitting leads to $\zeta_{g1,4}$ and $\zeta_{g1,2}$ in Figure 8 as a function of composition $\phi_{1,4}$ in both object and mirror systems. Here $\zeta_{g1,4}$ at $\phi_{1,4} = 1$, obtained by fitting eq 1 to $\zeta_{o1,4}$ in Figure 6a and $\zeta_{g1,2}$ at $\phi_{1,2} = 1$, obtained by fitting eq 1 to $\zeta_{o1,2}$ in Figure 6b, are nearly identical, as the flat line of ζ_{g0} indicates. This implies that ζ_g would approximately equal $\zeta_{g1,4}(\phi_{1,4}=1) \cong \zeta_{g1,2}(\phi_{1,2}=1)$ at all compositions in both systems when evaluated at their *true* glass transition temperatures $T_g(\phi)$. The drastic departure from ζ_{g0} in Figure 8 indicates that T_g^{DSC} may be significantly different from the true glass transition temperatures

Table 2. WLF Fitting Parameters for the Object and Mirror Solutions

object solutions				mirror solutions			
sample	c_1	c_2 (°C)	T_{gA} (°C)	sample	c_1	c_2 (°C)	T_{gB} (°C)
1,4-PB	11.8	48.2	−95.4	1,2-PB	11.6	50.8	−23.3
75% 1,4-	11.9	52.0	−91.0	75% 1,2-	12.6	67.1	−44.0
50% 1,4-	12.2	57.5	−85.5	50% 1,2-	12.9	78.0	−66.3
25% 1,4-	12.1	53.0	−69.4	25% 1,2-	12.3	67.5	−78.8

$T_g(\phi_{1,4})$ as felt by each component. Specifically, the fact that $\zeta_{g1,2} \gg \zeta_{g0}$ suggests that the 1,2- component is below its glass transition at T_g^{DSC}, where $\zeta_{g1,2}$ is evaluated. The increase of ζ_{g12} with $\phi_{1,4}$ further points out that the difference between $T_g^{DSC}(\phi_{1,4})$ and $T_{g1,2}(\phi_{1,4})$ grows with $\phi_{1,4}$. Similarly, the fact that $\zeta_{g1,4} \ll \zeta_{g0}$ indicates that the 1,4-component is above its glass transition at T_g^{DSC}. The difference between T_g^{DSC} and $T_{g1,4}$ apparently grows, driving $\zeta_{g1,4}$ to increase with $\phi_{1,4}$, as shown in Figure 8.

It is clear from the preceding analysis and discussion that T_g^{DSC} is not the true glass transition temperature for either component. Since $\zeta_g(\phi)$ is expected to be independent of ϕ and can be taken as ζ_{g0}, it is more reasonable to fit the data in Figure 6b−d using a second method by allowing c_1, c_2, and $T_g(\phi)$ to be adjustable in eq 1. The values for $T_g(\phi)$ that best fit the data are expected to represent the true glass transition temperatures possessed by each component. Figure 9a,b shows the fits obtained using the parameters listed in Table 2. We find that the best fits yield different T_gs for each of the two components. Moreover, the new $T_g(\phi)$ obeys the trends relative to T_g^{DSC} that were anticipated in our analysis of Figure 8 (see Figure 12a,b). It is worth noting that a similar conclusion made on a different basis for a different mixture has been reached previously.[15]

The approximate independence of $\zeta_g(\phi)$, c_1, and c_2 on composition ϕ leads us to consider shifting the data in Figure 9a,b to form two master curves as shown in Figure 10a,b. The temperature shifts $\Delta T(\phi)$ relative to the pure components are −6 (75%), −14 (50%), and −25 °C (75%) for the object systems and +16 (75%), +31 (50%), and +46 (25%) for the mirror systems, where minus means shifting data to the left and plus indicates a shift to the right-hand side. These shifts are *another* measure of where the true glass transition temperatures T_g' might be for each component at the different compositions.

Figure 9a,b shows that the 1,2-component has a stronger composition dependence. This can be seen in Figure 11a, illustrating the composition dependence of $\zeta_{1,2}$ and $\zeta_{1,4}$ at 20 °C. In other words, $\zeta_{1,2}$ decreases with decreasing $\phi_{1,2}$ more strongly than $\zeta_{1,4}$ decreases with increasing $\phi_{1,4}$. According to eq 1, the composition dependence arises primarily from that of their glass transition temperatures $T_{gA}(\phi)$ and $T_{gB}(\phi)$. Since the c_1 and c_2 for both components are similar, the discrepancy in the composition dependence appears to originate from the difference between $T_{gA}(\phi)$ and $T_{gB}(\phi)$. In other words, at any given temperature, the 1,2-component is closer to its true glass transition temperature $T_{gB}(\phi)$ than 1,4-component does so that $\zeta_{1,2}$ is more strongly affected by the composition change.

It is instructive to link our work with previous studies. In particular, we can also present the friction parameters in a manner following Kramer and coworkers.[15,16] If we plot $\zeta_{1,2}$ and $\zeta_{1,4}$ according to Figure 9a,b at a fixed distance from T_g^{DSC} (63 deg above) as a function of composition, we see that $\zeta_{1,2}$ (full squares) increases rapidly with $\phi_{1,2}$ and even exhibits a maximum and $\zeta_{1,4}$ (full circles) decreases below $\zeta_{01,4}$ with lowering $\phi_{1,4}$ as shown in Figure 11b. In other words, their ranges are not bounded by the respective values $\zeta_{01,2}$ and $\zeta_{01,4}$ of the pure components. Similar behavior, i.e., increase of both component friction coefficients with composition of the low-T_g component (i.e., $\phi_{1,4}$), has been reported before.[15] It is unreasonable to have $\zeta_{1,2} > \zeta_{01,2}$ and $\zeta_{1,4} < \zeta_{01,4}$ at a fixed distance from T_g^{DSC} unless T_g^{DSC} is not the true glass transition temperature. If $\zeta_{1,2}$ and $\zeta_{1,4}$ are evaluated at $T - T_g'$, where T_g' is the glass transition temperature according to the shifts performed in Figure 10a,b, we obtain the open symbols in Figure 11b that hardly vary with $\phi_{1,2}$ or $\phi_{1,4}$. Therefore, we believe that the strong composition dependence (full symbols) in Figure 11b arises from use of unrealistic glass transition temperatures for each component at different compositions. In other words, whenever one observes a strong increase of a friction coefficient with an increase in the low T_g in a mixture at a fixed $T - T_g(\phi)$, $T_g(\phi)$ is likely not the true glass transition temperature for the corresponding component.

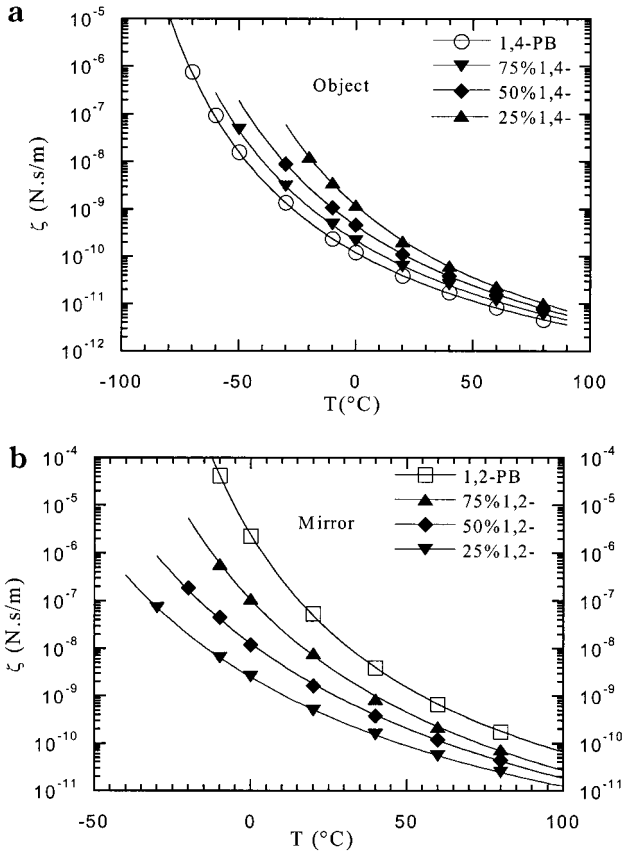

Figure 9. (a) Temperature dependence of friction coefficient of 1,4-PB in object solutions at different compositions. (b) Temperature dependence of friction coefficient of 1,2-PB in mirror solutions at different compositions. Here symbols are the data, and solid lines are the fit according to the parameters listed in Table 2.

Free Volume Theory for Mixtures. Free volume theory (FVT) has been applied successfully to provide a phenomenological account of the empirically established WLF relation although the microscopic origin of free volume remains to be identified. The concept of free volume is reasonably straightforward in a single-component polymer such as a pure melt. Fujita[17] extended the original FVT to describe polymer and

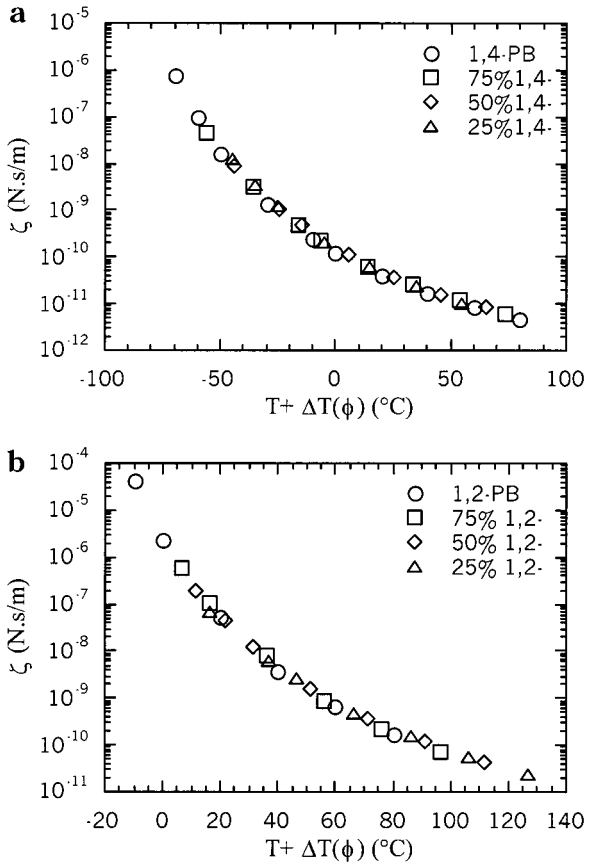

Figure 10. Horizontal shifts $\Delta T(\phi)$ (see the text for their actual values) of data in Figure 9a,b for (a) object and (b) mirror systems.

solvent dynamics in polymer solutions. However, the free volume fraction f felt by both solvent and polymer was assumed to be identical, and the logarithmic friction coefficients for both were taken as proportional to $1/f$.

In a uniform polymer mixture of different chemical species, it is unreasonable to assign the same free volume fraction to the different components. On the other hand, a common free volume is convenient because it provides the basis for a single glass transition for the mixture. Our data and corresponding analysis suggest that the broadening of the glass transition as observed in DSC of the polybutadiene mixtures may reflect sequential transitions of the respective PB of high vinyl content and low vinyl content. This possible scenario can be readily described within the framework of FVT by allowing each component to experience a different amount of free volume. According to the classical FVT for a mixture, the common f is given in terms of the free volume fractions f_{A0} and f_{B0} of the pure components as[18]

$$f = \phi f_{A0} + (1-\phi) f_{B0} + \kappa\phi(1-\phi), \qquad f_{A0} = f_g + \alpha_{A0}(T - T_{gA0}), \qquad f_{B0} = f_g + \alpha_{B0}(T - T_{gB0}) \quad (2)$$

where κ is an empirical parameter accounting for any coupling effect and the other parameters assume their usual meanings in the standard FVT. In our mixtures, let us allow the 1,4- and 1,2-components to have their own free volume fractions f_{14} and f_{12}, respectively. Below we use the more general notation A and B to label the two components in a mixture. f_A may differ from f and f_B. The following simple expressions account for f_A and

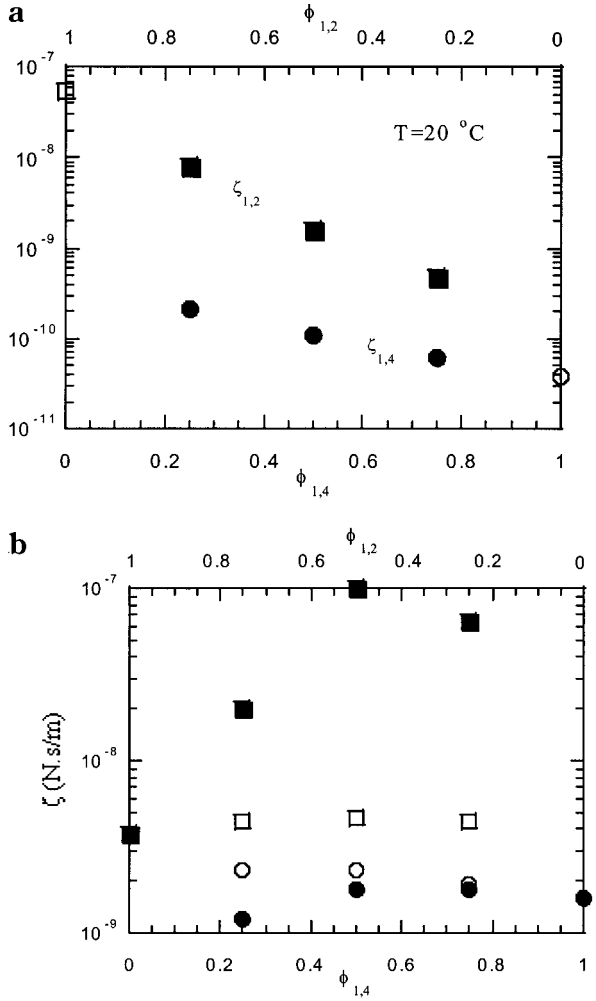

Figure 11. (a) Comparison of friction coefficients at a given temperature, where the open symbols come from rheological measurements of the pure components. (b) Friction coefficients of 1,4-component (circles) and 1,2-component (squares) as a function of composition ϕ at 63 °C from either T_g^{DSC} determined by the DSC (full symbols) or the shifts (open symbols) according to Figure 10a,b, i.e., at $T - T_g^{DSC} = 63$ (full) or $T - T_g' = 63$ °C (open). In both (a) and (b), squares obtained from the mirror solutions should be read with respect to the composition $\phi_{1,2}$ of 1,2-PB at the top abscissa. The circles are from the object system with respect to $\phi_{1,4}$ of 1,4-PB at the lower abscissa.

f_B deviations from f that are proportional to ϕ and $(1-\phi)$, respectively:

$$f_A = f + a\phi(f_{A0} - f) \quad (3a)$$

$$f_B = f + b(1-\phi)(f_{B0} - f) \quad (3b)$$

According to eq 3a and eq 3b, when $\phi = 1$, both f_A and f_B become f_{A0}. Similarly when $\phi = 0$, both become f_{B0}. The coupling constants a and b describe how f_A and f_B deviate from a common f, with $a = b = 1$ representing maximum deviations. Since $T_{gA0} < T_{gB0}$, we expect $(f_{A0} - f) > 0$, and the positive second term in eq 3a depicts plasticization by component A. On the other hand, $(f_{B0} - f) < 0$, and the negative second term in eq 3b denotes deplasticization by component B. The self-deplasticization is less effective, and we expect $b < 1$.

We can examine the consequences of eq 3a and eq 3b as follows. First, we fit the DSC data T_g^{DSC} from Figure 1c with the standard FVT: $f[T = T_g(\phi)] = f_g$. We find

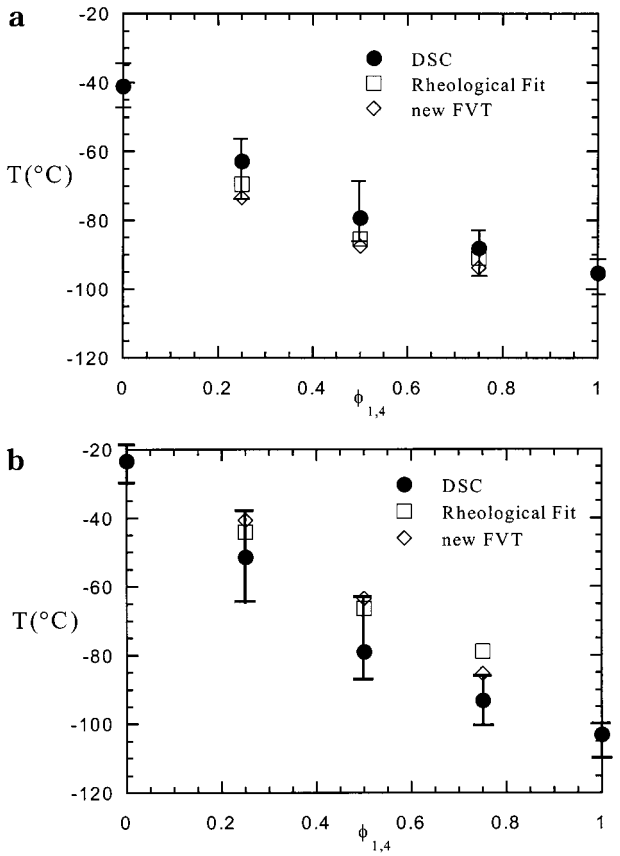

Figure 12. Comparison between glass transition temperatures obtained through the rheological curve shifting, DSC measurements, and description of the new free volume theory for both (a) object solutions and (b) mirror solutions, where the error bars indicate the width of the glass transition as determined by the DSC.

that $\alpha_{B0}/\alpha_{A0} = 0.6$ and $\kappa/\alpha_{A0} = 9$ give a good fit for the object system of 1,4-PB in 1,2-oBD. The same values are then used in eq 3a to obtain $T_{gA}(\phi)$ according to $f_A[T = T_{gA}(\phi)] = f_g$, where $a = 1$ is assumed. Figure 12a shows respectively three sets of data from DSC, rheological fit listed in Table 2, and the new FVT given in eq 3a. It is remarkable that the data from "new FVT" fall within the range of the glass transition indicated by the error bars.

It is found that $\alpha_{B0}/\alpha_{A0} = 0.5$ and $\kappa/\alpha_{A0} = 6$ fit well the data in Figure 1c for the mirror system of 1,2-PB in 1,4-oBD. The same values are then used in eq 3b to obtain $T_{gB}(\phi)$ according to $f_B[T = T_{gB}(\phi)] = f_g$, where $b = 0.7$ is used. Figure 12b shows respectively three sets of data for the mirror system from DSC, rheological fit listed in Table 2, and the new FVT given in eq 3b. It is worth noting that $b = 1$ would produce values of $T_{gB}(\phi)$ well outside of the transition width indicated by the error bars in Figure 12b.

As shown in Figure 11a,b, the new formulation of FVT systematically describes the trend of the individual glass transitions in agreement with the conclusions from the rheological analysis. The 1,4-component is suggested to possess a lower T_{gA} than that indicated by DSC at all compositions. Conversely, the 1,2-component is found to experience its glass transition at a higher temperature than that indicated by DSC. In other words, when lowering temperature, the 1,2-component is envisaged to undergo the glass transition before the 1,4-component takes its turn at a lower temperature. Thus, it is reasonable to visualize and interpret the observed broadening (see Figure 1a,b) of the glass transitions as due to the consecutive separate glass transitions of the two components in the mixtures.

V. Discussion and Conclusions

Component dynamics have been extensively studied in the past decade in search for an explanation for the thermorheological complexity, i.e., the breakdown of the time−temperature superposition principle in miscible polymer blends.[11,15,16,19−29] Various techniques have been applied to decouple the individual dynamics, including NMR,[11,28] rheology and birefringence,[23] quasi-elastic neutron scattering (QENS),[28] and dielectric spectroscopy.[28,29] In these studies, a great deal of attention has been paid to component dynamics on local length and therefore short time scales, often related to the α-relaxation processes. The existing techniques have their typical limitations. For the NMR method to differentiate individual component dynamics, the resonance lines of the two components cannot overlap. The QENS requires chemical labeling to increase the contrast between the components. Dielectric spectroscopy is selective only if the two components have very different molecular dipole moments. Often one is only able to investigate the effect of blending on dynamics of one of the two components.[28] It is highly desirable to correlate the more microscopic dynamic information on miscible blends with rheological measurements that contain information about the terminal relaxation dynamics. This bridging should be a central goal of future research.

In the present work, we are interested in probing the component dynamics associated with the terminal relaxation behavior because they are most relevant to understanding the processing behavior of polymer blends and establishing mixing rules for linear viscoelasticity. We developed a rheological means to resolve the component dynamics, which we call the solution rheology approach (SRA). Using SRA, we can separately evaluate the component dynamics of any miscible polymer blends from the terminal relaxation times in terms of their individual friction coefficients. SRA has several advantages. First, it is simple, universal, and inexpensive, involving no chemical labeling. Second, it allows component dynamics to be studied throughout the composition range, including the two-phase region because the component of short chains usually suppresses phase separation effectively. Third, it offers the explicit information on segmental friction coefficients as a function of composition and temperature. One shortcoming of SRA already showed up in the present article: the *unentangled* A (B) chains have a lower glass transition temperature than its entangled counterpart, thanks to the fact that T_g decreases with lowering molecular weight for oligomers. The principal reason for choosing unentangled B (A) oligomers to form entangled "solutions" with polymer A (B) is to simplify the data analysis. Here the rheological effect of short chains is merely to dilate the tube for chain reptation of the long chains. Until now, the influence of *entangled* short chains on the terminal relaxation time of a mixture of long and short chains remains elusive and will be the focus of our future publications.

In conclusion, the friction dynamics of each component in a mixture are found to exhibit different temperature and composition dependence on the largest length scale involving the overall reptation relaxation

dynamics. Specifically, the low-T_g component, i.e., 1,4-PB component, is found to have a weaker temperature dependence than that of 1,2-PB component at any given composition. Further analysis shows that this difference can be attributed to a difference in the true glass transition temperatures of the respective components. The high-T_g 1,2-component displays a much stronger composition dependence than 1,4-component does at all temperatures, especially at low temperatures. This can also be interpreted to arise from the true glass transition temperature of the 1,2-component being higher than that of the 1,4-component. Thus, we have inferred about the presence of different glass transitions in a miscible blend on the basis of the observed difference in the temperature dependence of the individual terminal dynamics at various compositions. The microscopic origins of *two* glass transitions in such a mixture are unclear, and our SRA is not designed to address this deeper issue.

Some of the presented observations have been made before for a similar system[23] and can be put in a similar context as the previous work did using diffusion measurements.[15,16] Comparison of the present results with those obtained with dielectric spectroscopy and QENS is less straightforward because these techniques typically examine the component dynamics at more microscopic scales. In general, a stronger difference is revealed; in other words, the component dynamics are less affected by blending and more heterogeneous, when examined with a more microscopic probe on shorter time scales.[28,29] As mentioned above, a bridge needs to be built between the long time viscoelastic relaxation processes and segmental relaxation processes such as the α-relaxation.

A comparison of two different data analyses presented in the preceding session urges us to abandon the old idea of a common glass transition temperature and leads us to propose a modified free volume theory allowing each component to experience a different level of free volume fraction in a mixture. Both new analysis and free volume theory show that the high-T_g component undergoes its glass transition at a higher temperature than that indicated by the DSC at all compositions. Conversely, the low-T_g component appears to undergo its glass transition at a lower temperature than that indicated by the DSC at all compositions. The traditional perception of a common free volume and glass transition for mixtures does not suit our data and requires a radical revision.

Acknowledgment. This work is supported, in part, by the National Science Foundation grants (CTS-9819704 and DMR-0074178). The generous provision of Rheometrics RMS-800 by Professor H. Ishida is gratefully acknowledged. Finally, we acknowledge the editorial comments by Dr. John T. Bender.

References and Notes

(1) Yang, X.; Wang, S. Q.; Ishida, H. *Macrmolecules* **1999**, *32*, 2638.
(2) De Gennes, P. G. *J. Chem. Phys.* **1971**, *55*, 572.
(3) Doi, M.; Edwards, S. F. *The Theory of Polymer Dynamics*; Clarendon Press: Oxford, 1986.
(4) Colby, R. H. *Polymer* **1989**, *30*, 1275.
(5) Lau, S.; Pathak, J.; Wunderlich, B. *Macromolecules* **1982**, *15*, 1278.
(6) Zetsche, A.; Kremer, F.; Jung, W.; Schulze, H. *Polymer* **1990**, *31*, 1883.
(7) Fischer, E. W.; Zetsche, A. *ACS Polym. Prepr.* **1992**, *33*, 78.
(8) Zetsche, A.; Fischer, E. W. *Acta Polym.* **1994**, *45*, 168.
(9) Kumar, S. K.; Colby, R. H.; Anastasiadis, S. H.; Fytas, G. *J. Chem. Phys.* **1996**, *105*, 3777.
(10) Kamath, S.; Colby, R. H.; Kumar, S. K.; Karatasos, K.; Floudas, G.; Fytas, G.; Roovers, J. E. *J. Chem. Phys.* **1999**, *111*, 6121.
(11) Lodge, T. P.; McLeish, T. C. B. *Macromolecules* **2000**, *33*, 5278.
(12) Chung, G. C.; Kornfield, J. A.; Smith, S. D. *Macromolecules* **1994**, *27*, 5729.
(13) Roovers, J.; Toporowski, P. M. *Macromolecules* **1992**, *25*, 1096.
(14) Fetters, L. J.; Lohse, D. J.; Richter, D.; Witten, T. A.; Zirkel, A. *Macromolecules* **1994**, *27*, 4639.
(15) Kim, E.; Kramer, E. J.; Osby, J. O. *Macromolecules* **1995**, *28*, 1979.
(16) Composto, R. J.; Kramer, E. J.; White, D. M. *Polymer* **1990**, *31*, 2320.
(17) Fujita, H. *Adv. Polym. Sci.* **1961**, *3*, 1.
(18) Ferry, J. D. *Viscoelastic Properties of Polymers*; Wiley: New York, 1980.
(19) Roland, C. M.; Ngai, K. L. *Macromolecules* **1991**, *24*, 2261.
(20) Roovers, J.; Toporowski, P. M. *Macromolecules* **1992**, *25*, 3454.
(21) Alegría, A.; Colmenero, J.; Ngai, K. L.; Roland, C. M. *Macromolecules* **1994**, *27*, 4486.
(22) Zawada, J. A.; Fuller, G. G.; Colby, R. H.; Fetters, L. J.; Roovers, J. *Macromolecules* **1994**, *27*, 6861.
(23) Arendt, B. H.; Krishnamoorti, R.; Kornfield, J. A.; Smith, S. D. *Macromolecules* **1997**, *30*, 1127.
(24) Mansour, A. A.; Madbouly, S. A. *Polym. Int.* **1995**, *36*, 269; **1995**, *37*, 267.
(25) Arrighi, V.; Higgins, J. S.; Burgess, A. N.; Howells, W. S. *Macromolecules* **1995**, *28*, 4622.
(26) Flores, R.; Perez, J.; Cassagnau, P.; Michel, A.; Cavaille, J. Y. *J. Appl. Polym. Sci.* **1996**, *60*, 1439.
(27) Mukhopadhyay, R.; Alegría, A.; Colmenero, J.; Frick, B. *J. Non-Cryst. Solids* **1998**, *235−237*, 233.
(28) Cendoya, I.; Alegría, A.; Alberdi, J. M.; Colmenero, J.; Grimm, H.; Richter, D.; Firck, B. *Macromolecules* **1999**, *32*, 4065.
(29) Arbe, A.; et al. *Macromolecules* **1999**, *32*, 7572.

MA0019306